

CHAPTER 64

Development of a Partially Three-Dimensional Model for Ship Motion in a Harbor with Arbitrary Bathymetry

Takumi Ohyama ¹ and Mitsuru Tsuchida ²

Abstract

A numerical method has been developed for the analysis of ship motions in a harbor with arbitrary bathymetry. A BEM-based 3-D model, applied partially to a near-field surrounding a ship, is combined with a FEM-based 2-D model, utilized in the remainder of harbor domain. This combination may achieve an efficient computation of the ship motions with taking into account of wave deformation in a harbor. Preliminary examinations have been performed to investigate appropriate location of a matching boundary where these two models are coupled. It is found that, for reliable prediction, $(2 \sim 3)h$ (h : water depth) is required for the distance between the matching boundary and a body. The numerical results of added mass and damping coefficients for a rectangular floating body in a rectangular basin are then compared with those obtained from a conventional numerical model. Favorable agreement between the results verifies the present numerical method. Ship motions in a harbor with slowly varying depth are also demonstrated.

¹Centre for Water Research, The University of Western Australia, Nedlands, WA6009, AUSTRALIA (on leave from Institute of Technology, Shimizu Corporation, Etchujima 3-4-17, Koto-ku, Tokyo 135, JAPAN)

²Institute of Technology, Shimizu Corporation, Etchujima 3-4-17, Koto-ku, Tokyo 135, JAPAN

1. Introduction

Precise prediction of ship motions in a harbor is essential to reliable harbor design. Coastal structures such as breakwaters and bottom topography in a harbor cause incoming waves to be diffracted and refracted before their reaching a floating body. In addition to such deformation of incoming waves, diffracted and radiated waves propagating from the body may be re-reflected by breakwaters and come back to the body again. Therefore, in general, hydrodynamic forces acting on a floating body in a harbor significantly differ from those in the case of open sea.

Under such circumstances, it may be necessary that the wave-ship interaction problem is solved simultaneously with the wave deformation in a harbor. In spite of this, corresponding numerical models, taking into account of coastal structures and bottom topography, have rarely been provided for predicting ship motions in a harbor. Oortmerssen (1976) developed a numerical method to calculate wave-induced motions of a ship moored at a straight quay, whereas Sawaragi and Kubo (1982) applied a two-dimensional boundary element method (2-D BEM) to the case of a rectangular floating body in a rectangular harbor. These basic studies may indicate essential influences of harbor boundaries on the ship motions. However, since these approaches have utilized the principle of mirror image, their applications are limited to harbors with straight boundaries.

In the light of this, Sawaragi et al. (1989) proposed a numerical method applicable to harbors of an arbitrary horizontal configuration. In their approach, a 3-D BEM model using a Green's function derived by John (1950) is applied only to the near-field around a floating body, and is combined with a 2-D BEM model utilized in the remainder of harbor domain. Although the basic idea of this "partially three-dimensional model" may address more practical situations as compared to the aforementioned methods, its application is still restricted to the case of constant depth in a harbor.

In this connection, the present study attempts to develop an alternative "partially three-dimensional model" for more general situations with a slowly varying bottom. A finite element method (FEM) based on the mild-slope equation (Berkhoff, 1972) is employed as a 2-D model in a harbor domain excluding the near-field around a floating body. Taking into account of continuities of fluid mass and momentum, this 2-D FEM model is coupled with a 3-D BEM model in the vicinity of the body.

The basic theory and the numerical formulation are described in Section 2, where the 3-D BEM and 2-D FEM models are solved simultaneously with continuity conditions imposed on a matching boundary. Since the 2-D model is

based on the mild-slope equation, this model is applicable only to the domain where evanescent modes are negligible. In this connection, Section 3 investigates an appropriate location of the matching boundary in a vertical two-dimensional plane. In Section 4, in order to verify the present numerical model, comparisons are made with a conventional model (Sawaragi and Kubo, 1982) for radiation-force coefficients of a rectangular floating body in a rectangular basin. Lastly, a numerical example is given in Section 5 for ship motions in a harbor with an inclined bottom.

2. Partially Three-dimensional Numerical Model

Governing equation and boundary conditions

Let us consider wave diffraction and radiation by a floating body in a harbor with arbitrary bathymetry. Assuming an irrotational small-amplitude motion of an incompressible and inviscid fluid, the fluid motion can be expressed by using the linear potential theory. The velocity potential for the wave-body interaction may be separated into the *propagation mode* and the *evanescent modes*, where the latter diminishes exponentially with distance away from the body. Therefore, in the present model, the harbor domain considered is subdivided into two regions, Ω_1 and Ω_2 , as shown in **Fig. 1**. The former region Ω_1 denotes a small near-field around the floating body where the evanescent modes are significant, whereas the latter Ω_2 represents a whole domain in a harbor excluding Ω_1 . It is assumed that the matching boundary, S_C , between Ω_1 and Ω_2 is located sufficiently apart from the body and, hence, only the propagation mode is predominant in Ω_2 .

The velocity potential, $\Phi(x, y, z, t)$ can be expressed by the combination of incident, diffraction and radiation potentials:

$$\Phi(x, y, z, t) = \phi_7(x, y, z)e^{-i\sigma t} + \sum_{l=1}^6 \frac{d}{dt}(D_l e^{-i\sigma t})\phi_l(x, y, z), \quad (1)$$

where (x, y, z) represents Cartesian coordinates (see **Fig. 1**), t is the time, σ is the angular frequency of incident waves, $l = 1, 2, \dots, 6$ correspond to the surge, sway, heave, roll, pitch and yaw body motions, respectively, ϕ_7 is the sum of incident and diffraction potentials, and ϕ_l and D_l ($l = 1 \sim 6$) are the radiation potential and the complex amplitude of the l -th directional body motion.

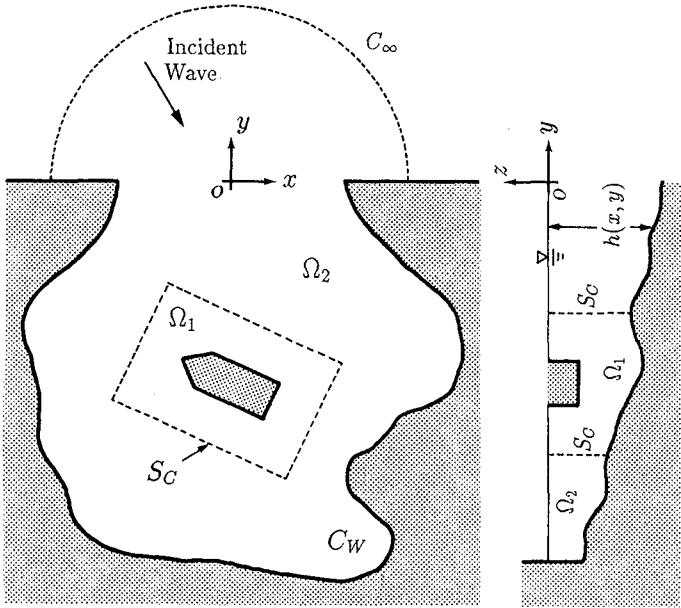


Fig. 1 Schematic diagram of partially three-dimensional model.

The governing equation and the boundary conditions for ϕ_l ($l = 1 \sim 7$) are

$$\frac{\partial^2 \phi_l^{(i)}}{\partial x^2} + \frac{\partial^2 \phi_l^{(i)}}{\partial y^2} + \frac{\partial^2 \phi_l^{(i)}}{\partial z^2} = 0, \quad (l = 1 \sim 7; \text{ in } \Omega_1 [i = 1] \text{ and } \Omega_2 [i = 2]), \quad (2)$$

$$\frac{\partial \phi_l^{(i)}}{\partial z} - \frac{\sigma^2}{g} \phi_l^{(i)} = 0, \quad (l = 1 \sim 7, i = 1, 2; \text{ on } S_F), \quad (3)$$

$$\frac{\partial \phi_l^{(i)}}{\partial n} = 0, \quad (l = 1 \sim 7, i = 1, 2; \text{ on } S_B), \quad (4)$$

$$\frac{\partial \phi_l^{(1)}}{\partial n} = v_l, \quad (l = 1 \sim 7, \text{ on } S_V), \quad (5)$$

$$\left. \begin{aligned} v_1 &= n_x, v_2 = n_y, v_3 = n_z, \\ v_4 &= (y - y_G)n_z - (z - z_G)n_y, \\ v_5 &= (z - z_G)n_x - (x - x_G)n_z, \\ v_6 &= (x - x_G)n_y - (y - y_G)n_x, \\ v_7 &= 0, \end{aligned} \right\} \tag{6}$$

where $\phi_i^{(1)}$ and $\phi_i^{(2)}$ denote the velocity potentials in Ω_1 and Ω_2 , respectively, S_F is the free surface, S_B is the seabed, S_V is the submerged body surface, n is the outward normal on each surface, (n_x, n_y, n_z) are the x -, y - and z -components of the outward unit normal on S_V , and (x_G, y_G, z_G) is the gravitational center of the body.

On the other hand, partial wave reflection is considered along the harbor boundary C_W . Although Isaacson and Qu (1990) proposed a corresponding boundary condition including the effects of wave direction and phase shift, the present study utilizes the following simple condition:

$$\frac{\partial \phi_i^{(2)}}{\partial n} = \frac{i\sigma}{C} \frac{1 - K_{RW}}{1 + K_{RW}} \phi_i^{(2)}, \quad (l = 1 \sim 7, \text{ on } C_W), \tag{7}$$

where C is the wave celerity and K_{RW} represents the reflection coefficient imposed.

3-D BEM model in Ω_1

Applying Green’s theorem to the fluid domain Ω_1 , the Laplace’s equation Eq. (2) is transformed into the following integral equation:

$$\alpha(P)\phi_i^{(1)}(P) + \int_S \left\{ \phi_i^{(1)} \frac{\partial G}{\partial n} - \frac{\partial \phi_i^{(1)}}{\partial n} G \right\} ds = 0, \quad (l = 1 \sim 7), \tag{8}$$

where S represents the closed boundary surface containing Ω_1 , P denotes an arbitrary position in Ω_1 , and G is a Green’s function. The coefficient $\alpha(P)$ is 2π if P is on S , and is 4π in other cases.

Using a Green’s function derived by John (1950) and substituting the boundary conditions, Eqs. (3), (4) and (5), into Eq. (8), the following boundary integral equations can be obtained:

$$\alpha(P)\phi_i^{(1)}(P) + \int_{S_C} \left\{ \phi_i^{(1)} \frac{\partial G}{\partial n} - \frac{\partial \phi_i^{(1)}}{\partial n} G \right\} ds + \int_{S_V \cup S_B} \phi_i^{(1)} \frac{\partial G}{\partial n} ds = \int_{S_V} v_l G ds, \tag{9}$$

(l = 1 ~ 7).

If the water depth is constant in Ω_1 , the integral on S_B involved in Eq. (9) can be eliminated since $\partial G/\partial n = 0$ (on S_B).

2-D FEM model in Ω_2

In Ω_2 , sufficiently far from the body, we may consider only the propagation mode in the fluid motion over a slowly varying seabed. This allows us to utilize the mild-slope equation (Berkhoff, 1972; Smith and Sprinks, 1975; Lozano and Meyer, 1976).

Thus, the velocity potential ϕ_l in Ω_2 is approximated by the form

$$\phi_l^{(2)}(x, y, z) = \varphi_l^{(2)}(x, y) \frac{\cosh k(h+z)}{\cosh kh}, \quad (l = 1 \sim 7), \quad (10)$$

where $k(x, y)$ and $h(x, y)$ are the wave number and the water depth, respectively. The corresponding mild-slope equation, derived from Eq. (2), is given as

$$\nabla \cdot (CC_G \nabla \varphi_l^{(2)}) + k^2 CC_G \varphi_l^{(2)} = 0, \quad (l = 1 \sim 7, \text{ in } \Omega_2), \quad (11)$$

where $\nabla \equiv (\partial/\partial x, \partial/\partial y)$ and C_G is the group velocity.

According to Chen and Mei (1975), a variational approach is employed in a FEM-based formulation to solve Eq. (11). Along the open boundary, denoted by C_∞ in **Fig. 1**, the finite elements are coupled to the *superelement* which satisfies the radiation condition analytically. The exterior region outside C_∞ is assumed to have a constant water depth.

The variational function for the governing equation [Eq. (11)], the boundary condition on C_W [Eq. (7)] and the radiation condition is given as

$$J_l = (J_1)_l + (J_2)_l + (J_3)_l + (J_4)_l, \quad (l = 1 \sim 7), \quad (12)$$

$$\left. \begin{aligned} (J_1)_l &= \int_{\Omega_2} \frac{1}{2} \left\{ CC_G (\nabla \varphi_l^{(2)})^2 - \frac{C_G}{C} \sigma^2 (\varphi_l^{(2)})^2 \right\} d\Omega, \\ (J_2)_l &= \int_{C_\infty} CC_G \left\{ \left(\frac{1}{2} \bar{\varphi}_l - \varphi_l^{(2)} + \frac{1}{2} \delta_{l7} \varphi_0 \right) \frac{\partial \bar{\varphi}_l}{\partial n} - \frac{1}{2} \delta_{l7} (\bar{\varphi}_l - \varphi_0) \frac{\partial \varphi_0}{\partial n} \right\} dc, \\ (J_3)_l &= - \int_{C_W} \frac{1}{2} i \sigma C_G \frac{1 - K_{RW}}{1 + K_{RW}} (\varphi_l^{(2)})^2 dc, \\ (J_4)_l &= - \int_{C_C} CC_G \frac{\partial \varphi_l^{(2)}}{\partial n} \varphi_l^{(2)} dc, \end{aligned} \right\} \quad (13)$$

where δ_{ij} is the Kronecker's delta, φ_0 is the velocity potential of incident waves, C_C is the intersection of the free surface and the matching boundary S_C , and $\bar{\varphi}_l$ denotes the exterior analytical solution (Chen and Mei, 1975).

Discretizing Eq. (12) by using linear triangular elements and applying the variational principle, we finally obtain a set of simultaneous equations for $\varphi_l^{(2)}$ in Ω_2 including C_C and $\partial \varphi_l^{(2)}/\partial n$ on C_C .

Continuity conditions on the matching boundary

The velocity potential, ϕ_l , and its normal derivative, $\partial\phi_l/\partial n$, must be continuous across the matching boundary S_C :

$$\phi_l^{(1)} = \phi_l^{(2)}, \quad \frac{\partial\phi_l^{(1)}}{\partial n} = \frac{\partial\phi_l^{(2)}}{\partial n}, \quad (l = 1 \sim 7, \text{ on } S_C). \quad (14)$$

Since the magnitude of evanescent modes is assumed negligible on S_C , these equations are rewritten by

$$\left. \begin{aligned} \phi_l^{(1)} &= \varphi_l^{(2)} \frac{\cosh k(h+z)}{\cosh kh}, \\ \frac{\partial\phi_l^{(1)}}{\partial n} &= \frac{\partial\varphi_l^{(2)}}{\partial n} \frac{\cosh k(h+z)}{\cosh kh} + \varphi_l^{(2)} \frac{\partial}{\partial n} \left(\frac{\cosh k(h+z)}{\cosh kh} \right), \end{aligned} \right\} (l = 1 \sim 7, \text{ on } S_C). \quad (15)$$

Substituting Eq. (15) into Eq. (9), we obtain

$$\begin{aligned} \alpha(P)\phi_l^{(1)}(P) + \int_{C_C} \left\{ \varphi_l^{(2)}(I_A - I_B) - \frac{\partial\varphi_l^{(2)}}{\partial n} I_C \right\} dc + \int_{S_V \cup S_B} \phi_l^{(1)} \frac{\partial G}{\partial n} ds, \\ = \int_{S_V} v_l G ds \quad (l = 1 \sim 7), \end{aligned} \quad (16)$$

where

$$\left. \begin{aligned} I_A &= \int_{-h}^0 \frac{\cosh k(h+z)}{\cosh kh} \frac{\partial G}{\partial n} dz, \\ I_B &= \int_{-h}^0 \frac{\partial}{\partial n} \left\{ \frac{\cosh k(h+z)}{\cosh kh} \right\} G dz, \\ I_C &= \int_{-h}^0 \frac{\cosh k(h+z)}{\cosh kh} G dz. \end{aligned} \right\} \quad (17)$$

Equation (16) is discretized into a finite number of facets on S_V and S_B , and of line elements on C_C . In the resultant discretized equation, the position of the control point P is set at the center of each element on S_V , S_B and C_C . This leads to $(N_V + N_B + N_C)$ linear algebraic equations involving $\phi_l^{(1)}$ (on S_V , S_B), $\varphi_l^{(2)}$ (on C_C) and $\partial\varphi_l^{(2)}/\partial n$ (on C_C) as unknown variables, where N_V , N_B and N_C are the number of elements on S_V , S_B and C_C , respectively. These equations are solved simultaneously with those obtained from the 2-D FEM model so as to determine the velocity potential in the both domains.

3. Location of the matching boundary

Prior to computing ship motions in a harbor, preliminary examinations are conducted to investigate the effect of the location of the matching boundary. As described in the previous section, the matching boundary must be set far enough away from the body so as to satisfy the assumption of negligible magnitude of evanescent modes.

For this examination, we consider a wave-diffraction problem in a vertical plane. In general, the horizontal variation of the magnitude of evanescent modes may be represented by

$$A_m e^{-k_m X}, (m = 1, 2, \dots),$$

where X denotes the horizontal distance from the origin of wave scattering, k_m is the m -th eigen value ($k_m \tan k_m h = -\sigma^2/g$), and A_m is a constant corresponding to the magnitude of the m -th mode at $X = 0$. Since $e^{-k_1 X} \geq e^{-k_2 X} \geq \dots$ ($k_1 < k_2 < \dots$), we may examine only the first mode, $A_1 e^{-k_1 X}$. The magnitude ratio of the first mode, normalized by A_1 , is then defined as

$$p(X) \equiv e^{-k_1 X}. \quad (18)$$

As an example, **Fig. 2** shows the computed reflection coefficient of a submerged rectangular shelf, K_R , for different values of p . In the figure, the abscissa denotes the normalized wave frequency, the solid line is the corresponding analytical solution obtained from an eigen-function expansion method, and S_R and S_T are the matching boundaries. The combination of a 1-D FEM model with a 2-D BEM model was employed for these computations.

As seen in the result for $p = 0.1$, a large value of p (small X) causes an apparent deviation from the analytical solution. In this case, the magnitude of evanescent modes may be still significant at the matching boundaries. While a slight discrepancy is observed for $p = 0.05$, the numerical results for $p = 0.01$ and 0.005 agree well with the linear theory in the entire frequency range examined, indicating that the assumption of negligible evanescent modes becomes appropriate.

In **Fig. 3**, the normalized distance, X/h_0 (h_0 : the water depth), is plotted for different values of p . It is found that X/h_0 corresponding to a constant p is insensitive to the wave frequency. The results shown in **Figs. 2** and **3** may conclude that the distance X , required for reliable prediction, is $2 \sim 3$ times as long as the water depth.

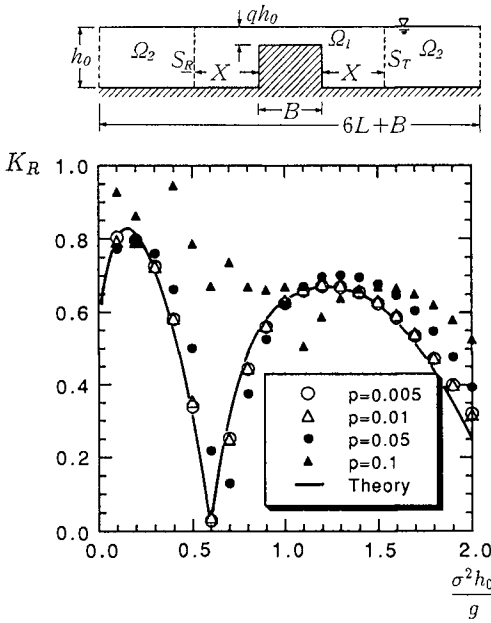


Fig. 2 Variation in computed reflection coefficients of a submerged rectangular shelf, with the location of matching boundaries.

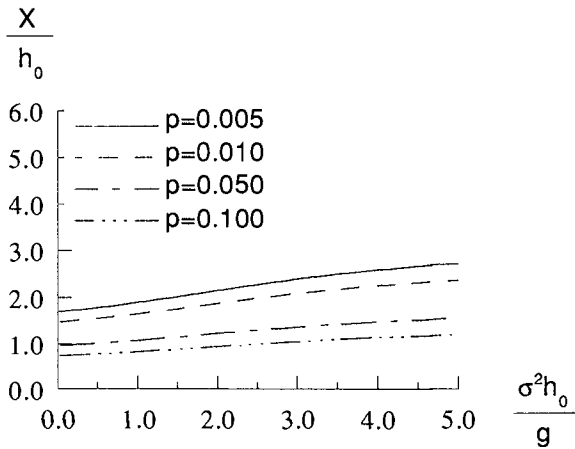


Fig. 3 Relation between the normalized distance X/h_0 and the parameter p .

For 3-D cases, the distribution of evanescent modes in a horizontal plane may be expressed as

$$B_{nm}K_n(k_m R) \cos n\theta, \quad (n = 0, 1, \dots, m = 1, 2, \dots),$$

where (R, θ) is local polar coordinates, B_{nm} is a constant and K_n is the modified Bessel function of the n -th order. Although the examinations were performed only in a vertical 2-D domain, the results obtained here may also be valid for 3-D cases since $K_n(k_m R)$ can be represented by using an exponential function $e^{-k_m R}$ for large R .

4. Comparison with a conventional numerical model

Sawaragi and Kubo (1982) computed hydrodynamic forces on a rectangular floating body in a rectangular basin by using a 2-D BEM model. Although the application of their model is limited to a rectangular harbor with a constant depth, the comparison with their results may confirm the validity of the present numerical model.

The numerical results for added mass and damping coefficients in the sway motion, M_{22} and N_{22} , are given in **Fig. 4**, where Δ and L_s are the weight and the length of the floating body. In the figure, the configurations of the basin and the floating body are also illustrated in a horizontal plane. The body's submergence and the water depth are $0.2m$ and $0.5m$, respectively, and the harbor boundaries are fully reflective ($K_{RW} = 1$).

As shown in this figure, predominant peaks of the hydrodynamic forces emerge at certain frequencies corresponding to harbor resonance. This peak phenomenon may suggest an importance of surrounding-boundary effects in predicting ship motions in a harbor. A favorable agreement between the results obtained from the present model and those from the 2-D BEM model (Sawaragi and Kubo, 1982) indicates the reliability of the present numerical model.

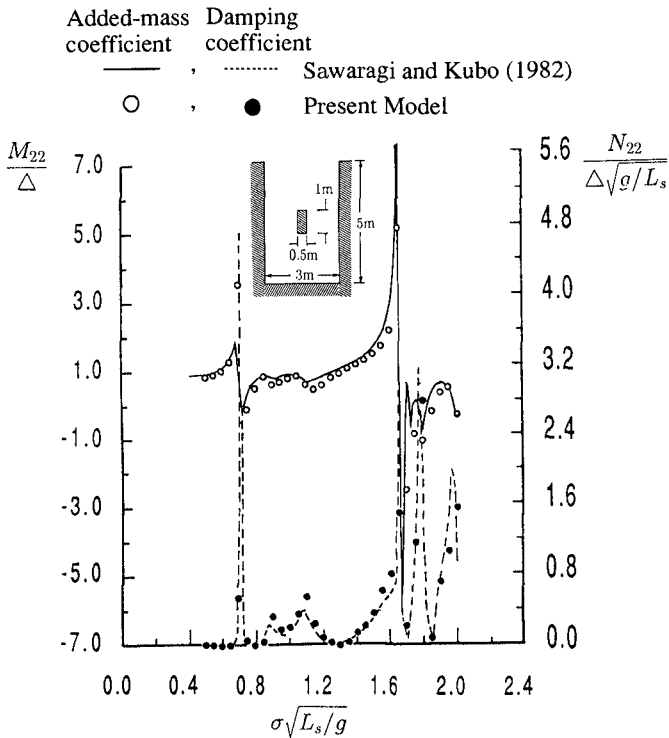


Fig. 4 Added-mass and damping coefficients in sway motion of a rectangular floating body in a rectangular basin.

5. Numerical Example

In addition to the influence of harbor boundaries, seabed topography may be one of the important factors for precise prediction of ship motions in a harbor. However, as mentioned in Introduction, most conventional approaches applied to this problem have assumed a constant water depth in a harbor. In this section, therefore, a numerical example is given for the case of a harbor with an inclined bottom.

The configurations of a floating body and a harbor examined are illustrated in **Fig. 5**. For reference, computations were also conducted for a flat-bottom case, for which the water depth is denoted by a broken line in this figure. The propagation direction of the incident waves is 30 degrees oblique to the harbor mouth.

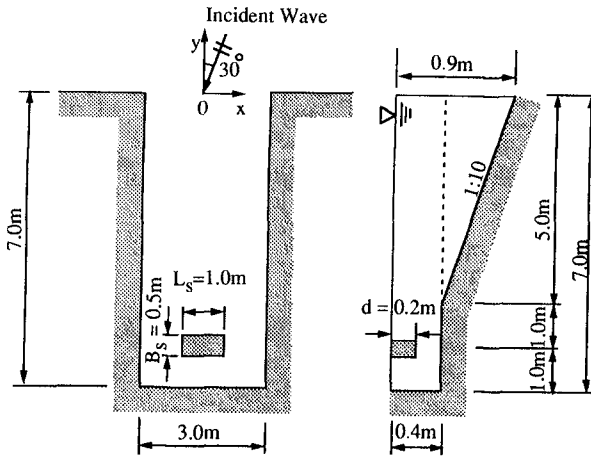
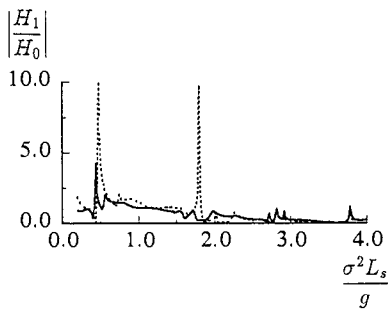
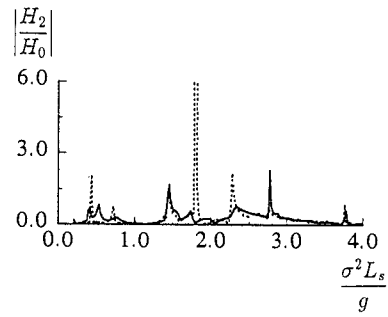


Fig. 5 Configurations of a floating body and a harbor examined.

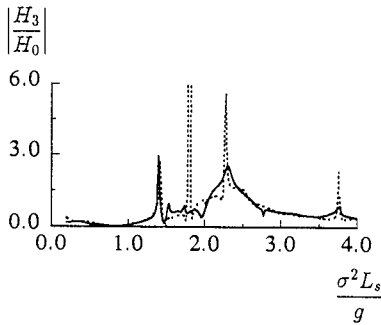
The resultant frequency responses of ship motions are shown in **Fig. 6**, where the solid and dotted lines represent the numerical results for the flat bottom and the inclined bottom, respectively, and H_0 is the incident wave height. Although resonant peaks emerge in the both numerical results, the corresponding peak frequencies are different between the cases. In particular, the computed responses for the inclined-bottom case shows distinctive peaks at $\sigma^2 L_s / g = 1.8$, which are not observed in the result for the flat-bottom case. This difference is attributed primarily to the variation in natural frequencies of the harbor. The results given in **Fig. 6**, therefore, may indicate an importance of a depth-variation effect on the ship motions in a harbor.



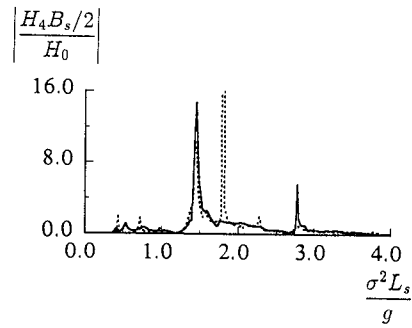
(a) Surge



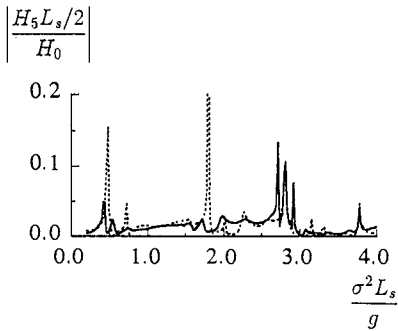
(b) Sway



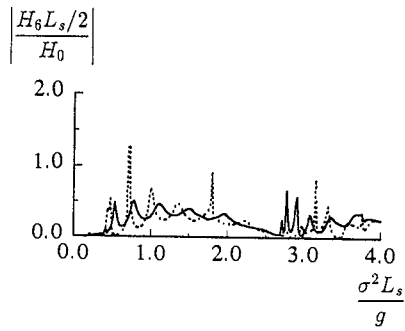
(c) Heave



(d) Roll



(e) Pitch



(f) Yaw

Fig. 6 Frequency responses of the ship motions for the flat-bottom case (———) and the inclined-bottom case (······).

6. Conclusions

A numerical method, composed of a BEM-based 3-D model and a FEM-based 2-D model, has been developed for the analysis of ship motions in a harbor with arbitrary bathymetry. This combination of the two different models may achieve efficient computation with taking into account of wave deformation in a harbor. Since the mild-slope equation is employed in a horizontal 2-D domain in a harbor, the present method can be applied to more general cases with varying water depth as compared to a conventional "partially 3-D model" (Sawaragi et al., 1989).

Basic examinations have been performed to investigate appropriate location of a matching boundary where the two models are coupled. The results show that, for reliable prediction, the distance between the matching boundary and a body is required to be $2 \sim 3$ times as long as the water depth. This practically satisfies a basic assumption that the magnitude of evanescent modes is negligible at the matching boundary.

The numerical results of radiation-force coefficients for a rectangular floating body in a rectangular basin are then compared with those obtained from a conventional method (Sawaragi and Kubo, 1982). Favorable agreement between the results verifies the present numerical method.

Lastly, ship motions in a harbor with an inclined bottom are demonstrated. The comparison between the numerical results for the flat-bottom and inclined-bottom cases indicates that the bottom topography may cause a variation in natural frequencies of harbor, which significantly influence the resultant ship motions.

References

- Berkhoff, J. C. W. (1972). "Computation of combined refraction-diffraction," *Proc. 13th Coastal Eng. Conf., ASCE*, 471-490.
- Chen, H. S. and C. C. Mei (1975). "Hybrid-element method for water waves," *Proc. the Modelling Techniques Conf.*, 1, 63-81.
- Isaacson, M. and S. Qu (1990). "Waves in a harbour with partially reflecting boundaries," *Coastal Eng.*, 14, 193-214.
- John, F. (1950). "On the motion of floating bodies II," *Comm. Pure and Appl. Math.*, 3, 45-101.

- Lozano, C. J. and R. E. Meyer (1976). "Leakage and response of waves trapped round islands," *Phys. Fluids*, **19**, 1075-1088.
- Oortmerssen, G. V. (1976). "The motions of a moored ship in waves," N.S.M.B. publication No.510, 1-138.
- Sawaragi, T. and M. Kubo (1982). "The motion of a ship in a harbor basin," *Proc. 18th Int. Conf. Coastal Eng., ASCE*, 2743-2762.
- Sawaragi, T., S. Aoki and S. Hamamoto (1989). "Analysis of hydrodynamic forces due to waves acting on a ship in a harbor of arbitrary geometry," *Proc. 8th Int. Conf. Offshore Mech. and Arctic Eng., ASME*, **2**, 117-123.
- Smith, J. D. and T. Sprinks (1975). "Scattering of surface waves by a conical island," *J. Fluid Mech.*, **72**, 373-384.